our present attitudes, we have used experimental data for three α-dicarbonyls which possess quite different CO/CO dihedral angles (θ = 0, 90, and 180°); we have adduced experimental arguments for heavy –C(O)C(O)– localization of excitation density in the low-energy $^1\Gamma_{n\pi^*} \leftarrow {}^1\Gamma_1$ transitions of these α-dicarbonyls; and, as a result, we feel secure in processing quantum chemical computations for glyoxals of variable θ and comparing the results so obtained to experimental data for diaromatic, monoaromatic, and wholly aliphatic α-carbonyls.

In the one-electron MO format, and using Koopmans' theorem, we have been able to rationalize[2] n_+ and n_- ionization potentials. We have also been able to conclude that the standard interpretation[1] (*i.e.*, $^1\Gamma_{n_+\pi^*} \leftarrow {}^1\Gamma_1$ and $^1\Gamma_{n_-\pi^*} \leftarrow {}^1\Gamma_1$) of the $S_1 \leftarrow S_0$ and $S_2 \leftarrow S_0$ transitions of the simple α-diketones is probably erroneous. This point of view is further vindicated by many-electron computations which include configuration interaction. However, while showing that the standard view has little to sustain it and that the interpretation advanced here is more consistent with the known facts, we do not wish to emphasize this facet of our work. Rather, we prefer to think that we have made a tentative start on a method which should eventually lead to a resolution of the problem posed. That is a study of energy levels, not solely at θ = 0, 90, and 180°, but over a wide range of θ. In addition, we believe further understanding will result from studies of such series as indanedione, 2,2,4,4-tetramethylcyclobutanedione, 1,4-cyclohexanedione, etc., where the two interacting loci, the >C=O groups, are not only made spatially separate but where the different symmetries also may impose considerably different selection rules on the various $^1\Gamma_{n\pi^*} \leftarrow {}^1\Gamma_1$ transitions.

Acknowledgment. This work was supported by contract between the U. S. Atomic Energy Commission (Division of Biomedical and Environmental Research—Physics and Technological Program) and the Louisiana State University. We wish to express our sincere thanks to Dr. Donald Larson (Rohm & Haas), for access to his comprehensive knowledge of α-dicarbonyl spectroscopy, and J. L. Meeks (Louisiana State University), for his extensive help in obtaining and interpreting photoelectron spectra.

Vapor Phase Excimer Formation in Saturated Amines

Arthur M. Halpern

Photochemistry and Spectroscopy Laboratory, Department of Chemistry, Northeastern University, Boston, Massachusetts 02115.
Received January 26, 1974

Abstract: The spectral and temporal properties of the excited state of the saturated amine, ABCO (1-azabicyclo-[2.2.2]octane), in the vapor phase are reported. On the basis of these properties, it is shown that ABCO forms an excimer in the vapor phase. This system is analyzed in terms of the usual monomer/excimer kinetic scheme to which one additional rate process had been added, the quenching of the excimer by ground state amine. The rate constants pertaining to the ABCO system are determined by measuring the monomer and excimer decay parameters as a function of the amine vapor pressure. The inference is drawn from solution phase studies that the ABCO excimer is strongly bound and is formed in the head-on approach of two ABCO molecules. The excimer formation efficiency in the vapor phase is determined to be *ca.* 0.2. The effects of added *n*-hexane vapor on the monomer and excimer emission efficiencies and kinetics are examined. Significant excimer enhancement is observed up to *n*-hexane overpressures of *ca.* 90 Torr. This is interpreted in terms of vibrational relaxation (and stabilization) within the monomer and excimer manifolds. The emission intensity and decay data imply that both radiative and nonradiative processes are induced by collisions between ABCO excited monomer and *n*-hexane molecules. The role of termolecular processes in excimer formation is suggested.

The association between ground and excited state molecules (excimer formation) is a well known phenomenon which occurs in the bimolecular electronic relaxation of many aromatic and heteroaromatic molecules.[1] It has been reported recently that certain saturated amines also undergo excimerization, both in the vapor phase and in solution.[2] It appears that vapor phase excimers have not been reported for the aromatic systems, presumably as a consequence of the low vapor pressures which characterize many excimer-forming aromatic molecules at ambient temperatures. At high temperature, where the vapor pressure is high enough to provide a sufficient collision frequency, the concomitant increase in the excimer dissociation rate results in a lower net excimer emission yield.[3]

It is of interest to study the dynamic and energetic properties of the excited monomer and dimer (*i.e.*, excimer) states in the absence of perturbing solvent molecules which affect both the formation and dissociation steps, as well as other nonradiative (and radiative) processes. This paper reports the results of a study of the ABCO, I (1-azabicyclo[2.2.2]octane), excimer in the vapor phase at ambient temperatures.

I

(1) J. B. Birks, "Photophysics of Aromatic Molecules," Wiley-Interscience, London, 1970, pp 301–371.

(2) A. M. Halpern and E. Maratos, *J. Amer. Chem. Soc.*, 84, 8273 (1972).

(3) B. Stevens and P. J. McCartin, *Mol. Phys.*, 8, 597 (1964).

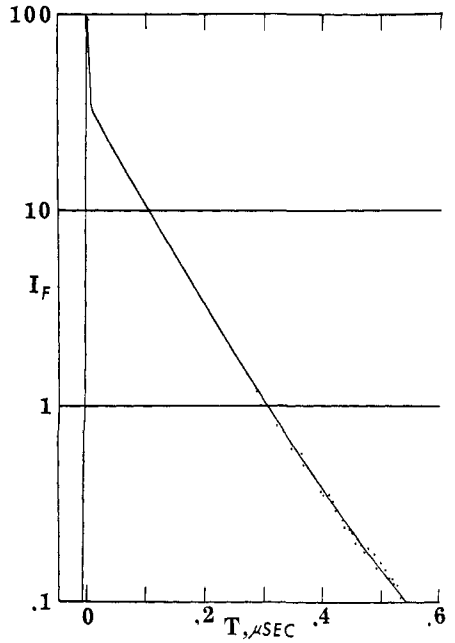

Figure 1. Decay curve for the ABCO monomer at 24°. The dots correspond to the experimental points and the solid line corresponds to the results of the convolution described in the text. Dots not indicated coincide with the line. Pressure is 2 Torr; λ_{exc} is 256 nm.

Experimental Section

ABCO was obtained and purified as reported in previous papers.[2,4] The fluorimeter and lifetime apparatus have also been described.[4,5] The vapor pressure of ABCO was determined at several temperatures using an MKS Baratron Model 77. These data are in good agreement with the results of Brown and Sujushi.[6] The vapor pressure of the amine was obtained by interpolating a $\log p$ *vs.* $1/T$ plot at appropriate temperatures. The temperature of the ABCO vapor was always between 24 and 28°, and the vapor pressure was set by having a small amount of the solid amine (in crystalline form) in a side arm attached to the fluorescence cell and immersed in a constant temperature bath.

In certain cases, in order to achieve higher signals (and reduce scattered light) in lifetime measurements, an all-quartz cylindrical cell (10 cm) was used. The cell was constructed from a Suprasil body with optically flat windows and the excitation axis coincided with the long axis of the cell. The entire cell was painted black, except for the excitation and emission windows.

For those experiments involving the addition of *n*-hexane vapor, the gas was added to a cell containing the solid amine, and the overpressure of the *n*-hexane was measured with a Wallace and Tiernan absolute pressure gauge. Measurements of the relative fluorescence intensity as a function of *n*-hexane pressure were made with the fluorescence cell fixed in the cavity of the fluorimeter, and the alkane vapor was admitted *via* the manipulation of external stopcocks. The associated vacuum rack was constructed with greaseless stopcocks.

For the fluorescence decay measurements, the ABCO monomer fluorescence was isolated using a Corion 2786-Å interference filter having a band pass of 180 Å, and the excimer emission was selected with a combination of Corning Glass 0-52 (7380) and 7-60 (5840) filters. The excimer fluorescence efficiency was determined by monitoring the intensity at 3750 Å (λ_{max}) as various pressures of thoroughly degassed *n*-hexane were added to the fluorescence cell. Since the monomer fluorescence is highly structured, its intensity was obtained by integrating the spectrum with a planimeter.

Results and Discussion

The fluorescence spectrum of ABCO vapor at ambient temperatures consists of two components. One of these is a highly structured vibronic system and extends from about 2500 Å to *ca.* 3200 Å. This has been assigned as fluorescence from the ABCO excited monomer state and has been described in ref 4. The other portion of the ABCO spectrum is a broad, structureless band with λ_{max} at about 3750 Å and extends to longer wavelengths out to about 4800 Å. This band has been assigned to the ABCO excimer emission on the basis of its concentration (pressure) dependence and its temporal properties.[2] The intensity of the excimer emission is observed to be strongly dependent on the pressure of a foreign gas (*e.g.*, *n*-hexane) added to the system as the ABCO partial pressure is held constant. The effects of *n*-hexane addition will be discussed below.

Kinetic Analysis

The ABCO vapor pressure was varied between 0.16 and 2.5 Torr. Over this pressure range, both the monomer and excimer fluorescence decay curves showed considerable changes. At higher pressures (*e.g.*, 1.95 Torr), the monomer decay curve was observed to be slightly nonexponential, and the extent of nonexponentially decreased as the vapor pressure was lowered. The time dependence of the ABCO (1.95 Torr) monomer fluorescence is shown in Figure 1. An analysis of this decay curve is presented below. The excimer decay curve possesses the expected build-up to maximum intensity, followed by a decay which gradually approaches an exponential dependence. An excimer decay curve for ABCO (1.95 Torr) is depicted in Figure 2. It will also be discussed below.

The fluorescence decay data are interpreted quantitatively within the framework of the following scheme. The designation of the rate constants follows the form used by Birks, *et al.*[7]

$$A \xrightarrow{h\nu} A^*$$

$$\left.\begin{array}{l} A^* \xrightarrow{k_{iM}} ? \\ A^* \xrightarrow{k_{fM}} A + h\nu_M \end{array}\right\} k_M$$

$$A^* + A \xrightarrow{k_{DM}} A_2^*$$

$$A_2^* \xrightarrow{k_{MD}} A^* + A$$

$$\left.\begin{array}{l} A_2^* \xrightarrow{k_{iD}} ? \\ A_2^* \xrightarrow{k_{fD}} A_2 + h\nu_D \end{array}\right\} k_D$$

$$A_2^* + A \xrightarrow{k_{QD}} ?$$

A, A*, and A_2* designate respectively the amine in the ground, excited monomer, and excimer states. k_M is the total of the excited monomer *uni*molecular relaxation rate constants (*i.e.*, radiative and nonradiative). k_{DM} and k_{MD} are the excimer formation and dissociation rate constants, respectively, and k_D represents the total unimolecular relaxation rate constants pertaining to the excimer *except* for dissociation. Finally, k_{QD} is the rate constant for the quenching of the excimer by ground state amine.

Solving the appropriate differential equations involving the disappearance rates of excited monomer and dimer provides the following results for the time

(4) A. M. Halpern, submitted for publication.
(5) A. M. Halpern and R. M. Danziger, *Chem. Phys. Lett.*, **12**, 72 (1972).
(6) H. C. Brown and S. Sujushi, *J. Amer. Chem. Soc.*, 70, 2878 (1948).
(7) J. B. Birks, D. J. Dyson, and I. H. Munro, *Proc. Roy. Soc., Ser. A*, **275**, 575 (1963).

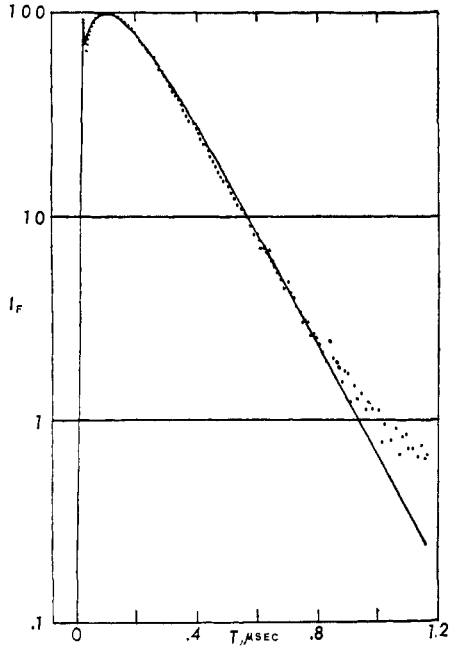

Figure 2. Decay curve for the ABCO excimer at 24°. The dots and the solid line have the same meaning as in Figure 1.

dependence of the monomer and excimer fluorescence intensities respectively (subsequent to δ pulse excitation)

$$I_{fM} \propto \exp(-\lambda_1 t) + A \exp(-\lambda_2 t) \quad (1)$$

and

$$I_{fD} \propto \exp(-\lambda_1 t) - \exp(-\lambda_2 t) \quad (2)$$

where

$$2\lambda_{1,2} = X + Y \mp \sqrt{(X - Y)^2 + 4k_{MD}k_{DM}c} \quad (3)$$

c is the concentration (in M) of ABCO vapor, and X, Y, and A are defined as

$$X = k_M + k_{DM}c$$

$$Y = k_D + k_{MD} + k_{QD}c$$

$$A = (X - \lambda_1)/(\lambda_2 - X)$$

The integrated fluorescence intensity functions, I_{fM} and I_{fD}, are identical with those published in ref 7 with the exception that $(X - Y)^2$ replaces $(Y - X)^2$ in the expression for $2\lambda_{1,2}$. This has no effect, of course, on values of $\lambda_{1,2}$ which are calculated for finite values of c, but this replacement is required in order that the proper limits of λ_1 and λ_2 are obtained as $c \rightarrow 0$. It is to be noted that the replacement of $(Y - X)^2$ by $(X - Y)^2$ has the same effect as switching the plus and minus signs in the expression for $\lambda_{1,2}$ as $c \rightarrow 0$. Thus, the limits of λ_1 and λ_2, as well as their respective slopes (*i.e.*, $\partial\lambda_{1,2}/\partial c$), as $c \rightarrow 0$ are reversed in this instance. This situation arises from the fact that $k_M > k_D + k_{MD}$, which is the opposite of the case for the pyrene system.[7]

The following parameters, then, can be identified with the monomer and excimer decay curves: λ_1 is the negative slope of ln (I_{fD}) *vs.* t at long times (see eq 2), and $I_{fM}(t)$ is represented by a sum of exponentials with time constants $-\lambda_1$ and $-\lambda_2$. At low pressures (below *ca.* 1 Torr), I_{fM} appears as a single exponential function

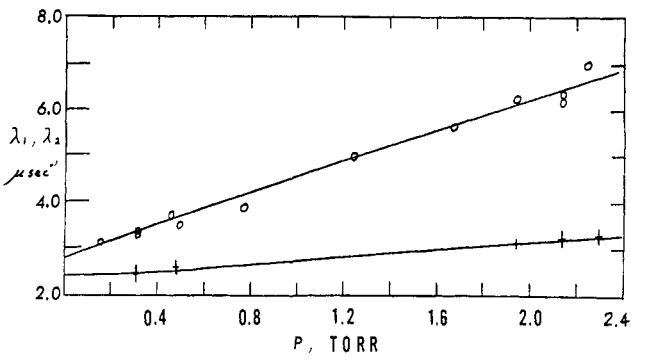

Figure 3. (○) Plot of λ_2 at various ABCO vapor pressures. The solid line drawn through these points corresponds to a plot of λ_2 *vs.* c calculated from eq 3 in which the rate constants used are listed in Table I. λ_{exc} is 256 nm. (+) Plot of λ_1 at various ABCO vapor pressures. The solid line drawn through these points is a plot of λ_1 *vs.* c calculated from eq 3.

in which the negative slope of ln (I_{fM}) *vs.* t is equal to λ_2. In principle, λ_2 can be obtained from the excimer decay curve by measuring the time required for I_{fD} to build up to a maximum and by directly determining λ_1 from the slope. The following expression would be utilized for this purpose

$$t_{max} = \ln(\lambda_2/\lambda_1)/(\lambda_2 - \lambda_1) \quad (4)$$

where t_{max} is the build-up time. This is not a very precise method for determining λ_2 because λ_2 is a rather insensitive function of t_{max} and λ_1. In the experiments reported in this paper, λ_2 was obtained directly from the monomer decay curve. Using the procedures described above, λ_1 and λ_2 were obtained for the ABCO monomer/excimer system at various pressures. These results are presented in the form of a plot of λ_1 and λ_2 as a function of ABCO vapor pressure in Figure 3.[8] At this point, a discussion of the expected slopes of these plots is pertinent. It can be shown that the limiting slopes of λ_1 and λ_2 *vs.* c (as $c \rightarrow 0$) are respectively

$$\left(\frac{\partial\lambda_1}{\partial c}\right)_{c\rightarrow 0} \equiv S_1 = k_{DM}\left(\frac{k_{MD}}{k_D + k_{MD} - k_M}\right) + k_{QD}$$

and

$$\left(\frac{\partial\lambda_2}{\partial c}\right)_{c\rightarrow 0} \equiv S_2 = k_{DM}\left(1 - \frac{k_{MD}}{k_D + k_{MD} - k_M}\right)$$

The intercepts are

$$\lim_{c\rightarrow 0} \lambda_1 = k_D + k_{MD}$$

and

$$\lim_{c\rightarrow 0} \lambda_2 = k_M$$

It is important to realize that these slopes are obtained in actuality at pressures below 0.2 Torr (*ca.* 10^{-5} M). At higher pressures (above *ca.* 0.4 Torr), the *observed* slopes correspond respectively to

$$S_1' = k_{QD} \quad (c > 2 \times 10^{-5}\ M)$$

$$S_2' = k_{DM} \quad (c > 2 \times 10^{-5}\ M)$$

It is to be noted that the justification for including the

(8) $\lambda_{1,2}$ values were obtained from experiments in which the exciting wavelength was 256 nm (the 0–0 band of the $S_1 \leftarrow S_0$ transition).

step for ground state amine quenching of excimer is based, in part, on the fact that $S_1' > 0$. The absence of such a quenching process would require that S_1' be equal to zero. Additional support for the requirement of a finite k_{QD} is presented below in connection with the decay curve analysis.

The solid lines shown in Figure 3 correspond to the calculated values of λ_1 and λ_2 as a function of concentration (pressure) (from eq 3). The departure from linearity can be noted at pressures below *ca.* 0.2 Torr. The rate constants used to calculate λ_1 and λ_2 are listed in Table I. k_{QD} and k_{DM} were obtained from the slopes

Table I. The Rate Constants Which Pertain to the Vapor Phase Excimerization of ABCO at 26° [a]

Rate constant	Value	Source
k_M	2.75×10^6 [b]	Intercept of λ_2 *vs.* vapor pressure plot
k_D	2.27×10^6 [b]	Intercept of λ_1 *vs.* vapor pressure plot; amplitude of λ_2 component in monomer decay
k_{MD}	1.3×10^5 [b]	Same as for k_D
k_{DM}	3.1×10^{10} [c]	Slope of λ_2 *vs.* vapor pressure plot
k_{QD}	8.4×10^9 [c]	Slope of λ_1 *vs.* vapor pressure plot

[a] λ_{exc} 256 nm. [b] sec^{-1}. [c] M^{-1} sec^{-1}.

of the experimental values of λ_1 and λ_2 plotted *vs.* pressure, respectively. The respective intercepts of these plots furnished values of $k_D + k_{MD}$ and k_M. The partitioning of the sum of excimer relaxation rate constants, k_D and k_{MD}, into the values indicated in Table I was accomplished by accurately measuring A, the relative amplitude of the λ_2 component in the monomer decay curve for a specific pressure. The decay curves shown in Figures 1 and 2 provide an example of the ability to determine A.

The dots correspond to the observed decay curve and the solid line to the convoluted decay curve to which a certain amount of scattered light (pumping function) was added, in order to reproduce properly the "spike" observed for the experimental decay curve. The convoluted function was of the form of eq 1, in which λ_1, obtained from an independent excimer decay curve, was constrained to a value of 3.12×10^6 sec^{-6} (*i.e.*, 1/(320 nsec)). λ_2, and its relative amplitude, A, were then varied until a satisfactory fit was obtained. The solid line shown in Figure 1 corresponds to the convoluted function in which λ_1 is as above, $\lambda_2 = 6.24 \times 10^6$ (*i.e.*, 1/(160 nsec)), and $A = 22$ (*i.e.*, 92% of the decay curve is represented by the λ_2 component). In Figure 1, the absence of a dot implies that it coincides with the solid line. It is estimated that the error in λ_2 is less than 1% and the error in A is roughly 10%.

According to the integral form of the decay law for the excimer emission (eq 2), the excimer decay curve should correspond to the difference of two exponential terms having equal amplitudes. The negative exponential component contains $-\lambda_2$ as the time constant. The appropriate excimer decay function for ABCO was convoluted with the exciting pulse profile, and a certain amount of this profile was then added to the convolution in order to reproduce the appearance of the spike observed in the excimer decay. Figure 2 illustrates this result. As in Figure 1, the dots correspond to the experimental data, and the solid line is the convoluted function plus scattered light. The observed build-up time, t_{max}, is consistent with the independently measured values of λ_1 and λ_2 and eq 4. It should be noted that a long-lived tail is observed in the excimer decay which cannot be accounted for on the basis of possible distortion by the exciting pulse. This effect is consistently observed and might conceivably be due to a long-lived emission component in ABCO vapor (*e.g.*, phosphorescence). The evacuated cell does not produce this effect. Phosphorescence has not been definitely observed in ABCO; however, weak, long-lived emission has been reported for ABCO at low temperature.[9]

The separation of k_M and k_D into their radiative (k_{fM}) and nonradiative (k_{iM}) parts cannot be done with reliability at this time. The quantum yield of monomer fluorescence has been estimated at near unity,[4] and k_{fM} would therefore be about 2.75×10^6 sec^{-1}. k_{iM}, presumably then, is very small. Since the excimer fluorescence efficiency is not known, estimates of k_{fD} and k_{iD} for the excimer are impossible to make.

The value of k_{DM}, the excimer formation rate constant, when compared with the hard-sphere collision rate constant (using an effective collision diameter of 6 Å), implies that p, the probability factor, is about 0.2. This is somewhat smaller than the corresponding value of p for ABCO in *n*-hexane solution.[10] It is certainly not surprising that $p < 1$ for the vapor phase system because an effective (*i.e.*, excimer-forming) collision requires the specific orientation of two encountering molecules. A comparison between the solution and vapor phase values of p would require explicit consideration of the difference in the nature excited states in these media, and in addition, one would have to take into account the cage effect in solution *vis-à-vis* binary collisions in the vapor phase.

It is interesting to note that k_{QD}, the rate constant for the ground state quenching of excimer, is considerably larger in the gas phase than in solution. In *n*-hexane, k_{QD} is about 4.6×10^7 M^{-1} sec^{-1}.[10] The reason for this large difference in k_{QD} values can probably be attributed to the fact that the nature of the excited monomer and excimer states in ABCO is different in these two media. For example, the lifetime of ABCO (monomer) in *n*-hexane (dilute solution) is *ca.* 55 nsec, which compares with 364 nsec for the zero-pressure extrapolated lifetime in the vapor phase. The solution and vapor phase excimer lifetimes are *ca.* 180 and 440 nsec, respectively.

An attempt was made to include in the expressions for λ_1 and λ_2 a rate constant which would account for the quenching of the excited monomer state by ground state amine (k_{QM}). However, both the monomer and excimer decay data, as well as the λ_1 and λ_2 *vs.* pressure plots, failed to support the inclusion of k_{QM} in the ABCO electronic relaxation scheme. Apparently, therefore, collisions between excited and ground state ABCO molecules either result in excimerization or are reversible (*i.e.*, ineffective in quenching the excited monomer).

Although the formation and dissociation rate con-

(9) Y. Muto, Y. Nakato, and H. Tsubomura, *Chem. Phys. Lett.*, 9, 597 (1971).

(10) R. J. Sternfels and A. M. Halpern, to be submitted for publication.

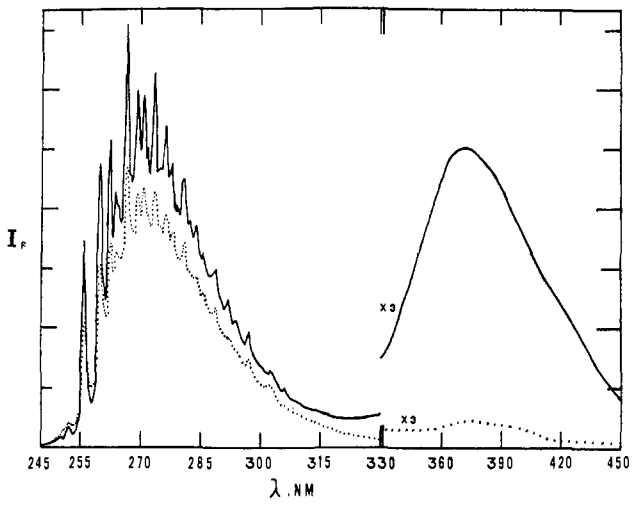

Figure 4. (···) Vapor phase emission spectrum of ABCO at 24°; the ABCO vapor pressure is 1.6 Torr. (—) The emission spectrum obtained after the addition of 90 Torr of *n*-hexane (same ABCO partial pressure). The exciting wavelength for both spectra is 228 nm.

stants are known for the ABCO excimer, thermodynamic parameters such as the entropy and enthalpy of formation cannot be directly calculated because the rate constants are determined from kinetic experiments under the condition in which the monomer and excimer states are *not* in equilibrium; *i.e.*, the rates of formation and dissociation are not equal. The binding energy of the excimer (which is $-\Delta H$) could be directly determined from photostationary state measurements at higher temperatures.[11] Alternatively, knowledge of the temperature coefficients of k_{MD} and k_{DM} can lead to the determination of the binding energy. However, if one assumes that the binding energy in the vapor phase can be approximated by the solution phase value, then $(\Delta H)_{vap} \simeq -10$ kcal/mol.[10] Thus, the ABCO excimer is rather strongly bound.

Using this estimated value for the binding energy, the repulsion energy, R, can be approximated. R is the amount of repulsion energy present in a pair of ground state ABCO molecules which possess the same geometry as the excimer. From spectroscopic considerations, R is determined from the following relation

$$E_{0-0}^{M} = B + R + E_{max}^{D}$$

where E_{0-0}^{M} is the S_1–S_0 energy of ABCO, B is the binding energy of the excimer, and E_{max}^{D} is the energy of maximum fluorescence intensity of the excimer. E_{0-0}^{M} is 39.078 cm^{-1} (2559 Å), E_{max}^{D} is 26,700 cm^{-1} (3750 Å) and R, therefore, is about 21 kcal/mol.[12] This implies that the two ABCO molecules approach each other rather closely in forming the excimer.

As will be discussed in a forthcoming publication,[10] the ABCO excimer forms in a "head-to-head" fashion, *i.e.*, with the two nitrogen atoms facing each other. INDO calculations[13] based on a rather simple model for the ABCO excimer system imply that a considerable amount of stability can be achieved from such an arrangement of amine molecules. These calculations were performed for a pair of trimethylamine molecules at various distances of approach along an axis which coincided with their C_3 axes. The amines approached each other head on and were constrained to possess normal ground state bond lengths and angles at all points along the reaction coordinate. One of the amines was in the ground state, while the other one was the radical cation $(CH_3)_3N\cdot^+$) in order to simulate the excited state.[14]

According to this calculation,[15] the energy of the radical cation is about 200 kcal/mol (9.4 eV) above the ground state and compares with the first adiabatic IP of trimethylamine of 7.80 eV.[16] Relative to zero energy for the pair of amines at large separation, a decrease in energy to a minimum value of −118 kcal/mol was obtained at a distance of *ca.* 1.6 Å between the two N atoms. The same calculation for a pair of two ground state molecules did not indicate the presence of an energy minimum. The energetics pertaining to a pair of ABCO molecules, one of which is in the lowest electronically excited state, would, of course, be entirely different quantitatively.

Pressure Effects

As indicated earlier, the excimer emission intensity is dependent upon the total pressure of the system. These effects are depicted in Figure 4 which shows the total ABCO emission spectrum with λ_{exc} of 228 nm. The ABCO partial pressure was kept constant at 1.6 Torr in this experiment. The dotted line is the ABCO spectrum with no foreign gas added, and the solid line is the spectrum produced when 90 Torr of *n*-hexane is introduced. The structured monomer fluorescence spectrum undergoes a slight enhancement as a result of this addition and will be discussed below.

As is evident from Figure 4, there is a very large enhancement in the excimer emission intensity. The effects of added *n*-hexane on the excimer emission intensity are illustrated in Figure 5 for *n*-hexane pressures of 0–150 Torr. In this figure, closed and open circles correspond respectively to excitation wavelengths of 228 and 249 nm. With λ_{exc} of 228 nm, there is an intensification of the excimer emission of about a factor of 10, relative to having no *n*-hexane vapor present, and this occurs at *ca.* 90 Torr. The maximum enhancement for λ_{exc} of 249 nm is about a factor of 4 at *ca.* 80 Torr. In both cases, the excimer intensity then decreases at pressures above 90 Torr.

These enhancement results can be thought of as a consequence of vibrational relaxation of the excimer immediately to its formation. Since the binding energy of the excimer is about 10 kcal/mol, it is at least this amount of vibrational energy which must be dissipated by the newly formed excimer. In other words, the excimer is stabilized when the formation enthalpy is adequately dissipated either among the internal degrees of freedom of the excimer or *via* collisions. Since the excimer contains 42 atoms, one would presume that

(11) B. Stevens and M. I. Ban, *Trans. Faraday Soc.*, **60**, 1515 (1964).

(12) This R value represents an upper limit if excimer fluorescence produces monomer molecules having energies larger than RT.

(13) J. A. Pople, D. L. Beveridge, and P. A. Dobosch, *J. Amer. Chem. Soc.*, **90**, 4201 (1968); D. L. Beveridge, P. A. Dobosch, and J. A. Pople, *J. Chem. Phys.*, 48, 4802 (1968).

(14) For Rydberg excited states, the limit corresponds to the cation, *i.e.*, $N\cdot^+$; see G. Herzberg, "Molecular Spectra and Molecular Structure III. Electronic Spectra and Structure of Polyatomic Molecules," Van Nostrand, Princeton, N. J., 1966, p 361 ff.

(15) Professor G. R. Underwood (New York University) is gratefully acknowledged for performing these calculations.

(16) A. N. Cornfield, D. C. Frost, F. G. Herring, and C. A. McDowell, *Can. J. Chem.*, **45**, 1135 (1971).

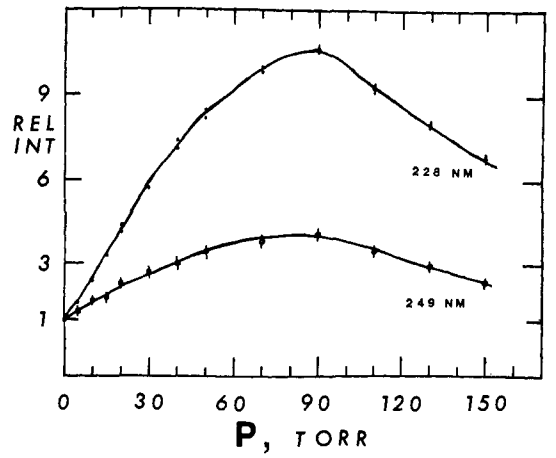

Figure 5. (●) Plot of the relative intensity of the excimer emission (monitored at 375 nm) at various overpressures of *n*-hexane. The exciting wavelength is 228 nm. (○) The same as above but with an exciting wavelength of 249 nm. The ABCO partial pressure is 1.6 Torr.

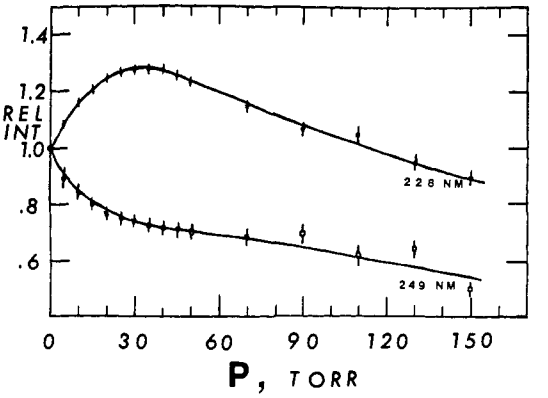

Figure 6. (●) Plot of the relative intensity of the monomer fluorescence intensity at various overpressures of *n*-hexane. The exciting wavelength is 228 nm. The ABCO partial pressure is 1.6 Torr. (○) The same as above but with an exciting wavelength of 249 nm.

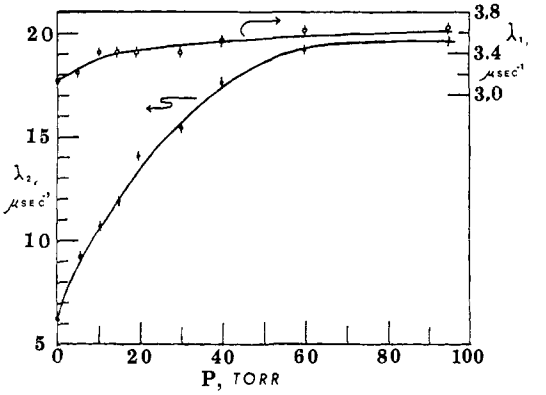

Figure 7. (●) Plot of λ_2 at various overpressures of *n*-hexane refers to left-hand axis. λ_{exc} is 256 nm. (○) Plot of λ_1 at various *n*-hexane overpressures refers to the right-hand axis. The ABCO partial pressure is 1.6 Torr. λ_{exc} is 256 nm.

there would be a sufficiency of oscillators in the system so that the excimer could act as its own "heat bath." The fact that such large enhancement effects are observed leads one to suspect that *intra*molecular vibrational energy transfer is impeded, perhaps as a result of the high molecular symmetry.

The fact that excimer fluorescence is observed in the absence of added *n*-hexane vapor implies that (1) the ABCO excimer, itself, is somewhat able to vibrationally relax *uni*molecularly and/or (2) that ground state ABCO molecules play a role in the vibrational relaxation of the excimer. A kinetic process such as in 2, above, has not been included in the kinetic scheme (*vide supra*). This exclusion is justified on the basis of (1) the ability to analyze the data in terms of *bi*molecular (emissive) excimer formation and (2) the fact that the maximum total ABCO pressure reached in the experiments was *ca.* 2.2 Torr, whereas the excimer fluorescence enhancement effects are observed at *n*-hexane pressures of *ca.* 80 Torr. Nevertheless, a more detailed analysis of the vapor phase kinetic data would include an appropriate *ter*molecular excimer formation process.

When the ABCO monomer is excited at energies above the $S_1(0\text{–}0)$ level, more energy must accordingly be dissipated by the excimer system. Thus, 228 nm (which coincides with the 0–0 band of the $S_2\text{–}S_0$ transition) lies about 8000 cm^{-1} above the excimer potential minimum. For 249 nm (the other excitation wavelength used in the experiments) this value is *ca.* 4400 cm^{-1}. The larger enhancement factor observed at 228 nm relative to 249 nm can be explained by that fact the extinction coefficient is considerably larger at 228 nm (the strongly allowed 0–0 band of $S_2 \leftarrow S_0$) than at 249 nm (which excites the weak $S_1 \leftarrow S_0$ transition).

The decrease in the excimer emission intensity observed at pressures greater than 90 Torr of *n*-hexane is a consequence of pressure effects on the ABCO's monomer excited state. The dependence of the monomer fluorescence intensity on the pressure of *n*-hexane is a consequence of pressure effects on the ABCO monomer excited state. The dependence of the monomer fluorescence intensity on the pressure of *n*-hexane vapor is illustrated in Figure 6 in which the two excitation wavelengths, 228 and 249 nm, are represented by closed and open circles, respectively. In these experiments, the relative fluorescence intensity was determined by integrating the structured $S_0 \leftarrow S_1$ spectrum and normalizing the results relative to the spectrum obtained with no *n*-hexane present. It is evident that one of the effects of the added gas is the inducement of vibrational relaxation within the S_1 manifold. This can be observed in Figure 4, in which some of the diffuseness in the spectrum (produced in the absence of *n*-hexane and with λ_{exc} if 228 nm) is removed. Moreover, several vibronic bands sharpen up considerably. This effect is also observed for λ_{exc} of 249 nm, but to a lesser degree. Therefore, the slight enhancement observed (λ_{exc} 228 nm) up to *ca.* 35 Torr is a result of vibrational relaxation and the consequential stabilization of the excited monomer.

An apparent quenching of the monomer fluorescence is observed with λ_{exc} of 249 as *n*-hexane is added. This is also seen at 228 nm at pressures greater than about 35 Torr. These effects are interpreted in terms of a pressure dependence in the radiative and nonradiative rate constants, k_{fM} and k_{iM}. This implies that collisions between ABCO in the excited state and *n*-hexane molecules are effective in inducing *both* radiative and nonradiative transitions. These effects are represented quantitatively in Figure 7. λ_2 (see eq 1 and 3) is indicated at various *n*-hexane pressures (λ_2 is denoted by the closed circles which refer to the left-hand axis). In

addition, λ_1, obtained from excimer decay curves, is shown in Figure 7 at several *n*-hexane pressures. For these data, open circles are used, and the right-hand axis pertains. The exciting wavelength used in these experiments was 2559 Å (the 0–0 band of $S_1 \leftarrow S_0$), and therefore vibrational relaxation effects (in the monomer manifold) would be very slight or absent.

From the data shown in Figure 7, the pressure coefficient of λ_2 (between 0 and 30 Torr) is about 6×10^9 M^{-1} sec^{-1}. Since the decrease in the monomer quantum yield indicated in Figure 6 for λ_{exc} of 249 nm is considerably less than the increase in λ_2 throughout the corresponding *n*-hexane pressure range, it can be concluded that both k_{fM} and k_{iM} are pressure dependent. The determination of the pressure coefficients of k_{fM} and k_{iM}, individually, is made rather difficult by the complexity of λ_2 (see eq 3), but, presumably, the pressure coefficient of k_{fM} is greater than that for k_{iM}. It is also possible that part of the increase in λ_2 (and the enhancement in the excimer emission intensity) can be attributed to increased excimer formation efficiency at higher *n*-hexane pressures (*i.e.*, a pressure-dependent k_{DM}). Thus, termolecular processes may be important in the ABCO excimer formation.

Observations of pressure dependent radiative and nonradiative rate constants in saturated amine systems have been made before. In these cases, the pressure coefficient of $1/\tau_f$ was also about 10^9 M^{-1} sec^{-1}. The apparently large (*n*-hexane) pressure dependence of k_{fM} may be a consequence of the Rydberg nature of the excited state(s) of saturated amines.[17,18] External pressure effects on the absorption spectra of Rydberg transitions have been examined by Robin and Kuebler[19] but at much higher pressures.

It is evident from Figure 7 that there is only a very slight effect on λ_1 by increasing the *n*-hexane pressure. This is a consequence of the diminished susceptibility of the excimer to collisional perturbation and implies that the excimer state is shielded because of the "head-to-head" configuration.

Acknowledgment. The author acknowledges with gratitude the support for this research by the donors of the Petroleum Research Fund, administered by the American Chemical Society. Mr. R. J. Sternfels is acknowledged for his assistance in devising useful computer programs. A referee is acknowledged for helpful comments.

(17) A. M. Halpern and T. Gartman, *J. Amer. Chem. Soc.*, **96**, 1393 (1974).
(18) A. M. Halpern, J. L. Roebber, and K. Weiss, *J. Chem. Phys.*, **49**, 1348 (1968).
(19) M. B. Robin and N. A. Kuebler, *J. Mol. Spectrosc.*, **33**, 274 (1970).

Gas Phase Thermal Decomposition of *tert*-Butyl Alcohol

David Lewis,* Mark Keil, and Michael Sarr

Contribution from Colgate University, Hamilton, New York 13346.
Received March 14, 1973

Abstract: The homogeneous, gas phase, thermal decomposition of *tert*-butyl alcohol to isobutene and water was studied in a single-pulse shock tube. The comparative rate technique was used, with the decyclization of cyclohexene to ethylene and 1,3-butadiene serving as the internal standard reaction. Over the temperature range 920–1175°K, the comparative rate data for unimolecular *tert*-butyl alcohol decomposition were fit well by the expression $\log k\ (sec^{-1}) = 14.6 - (66.2 \times 10^3/4.58T°K)$.

The gas phase thermal decomposition of *tert*-butyl alcohol has been the subject of a number of previous studies[1-4] (see Table I). Schultz and Kistiakowsky (S and K),[1] using a static reactor, determined that the primary reaction was the molecular elimination to form isobutene and water and that the reaction was first order down to 3 Torr, below which pressure falloff was encountered. Barnard,[2] working in a similar temperature and pressure range, obtained rate constants that agree with those reported by S and K at 760°K but which were considerably lower than those reported by S and K at higher temperatures. Thus his deduced activation energy value was lower (54.5 *vs.* 65.5 kcal). Tsang[3] studied the reaction at higher temperatures in a single-pulse shock tube and measured rate constants that fell between values predicted from extrapolation of S and K's and Barnard's Arrhenius plots. Dorko, *et al.*, have reported shock tube results essentially identical with Tsang's. Their study was run as a means of verifying proper operation of their shock tube in preparation for the study of other reactions. Workers in other laboratories[5,6] have also used this reaction for that purpose.

Table I. Results of Earlier Studies of *tert*-Butyl Alcohol Pyrolysis

T range, °K	*P* range, Torr	log *k*, sec^{-1}	Ref
760–828	1–344[a]	$14.68 - [(65{,}500 \pm 7{,}000)/4.58T°K]$	1
760–893	20–400	$(11.51 \pm 0.45) - [(54{,}500 \pm 1{,}700)/4.58T°K]$	2
1050–1300	*b*	$13.4 - [(61{,}500 \pm 4{,}300)/4.58T°K]$	3
b	*b*	$(13.35 \pm 0.20) - [(60{,}500 \pm 100)/4.58T°K]$	4

[a] Onset of falloff noted at about 3 Torr, at 789°K. [b] These data are not reported.

(1) B. F. Schultz and G. B. Kistiakowsky, *J. Amer. Chem. Soc.*, **56**, 395 (1934).
(2) J. A. Barnard, *Trans. Faraday Soc.*, **55**, 947 (1959).
(3) W. Tsang, *J. Chem. Phys.*, **40**, 1498 (1964).
(4) E. A. Dorko, D. B. McGhee, C. E. Painter, A. J. Caponecchi, and R. W. Crossley, *J. Phys. Chem.*, **75**, 2526 (1971).
(5) H. F. Carroll, Ph.D. Thesis, Cornell University, 1969.
(6) D. K. Lewis, Ph.D. Thesis, Cornell University, 1970.